Journal of Organometallic Chemistry, 399 (1990) 349–360
Elsevier Sequoia S.A., Lausanne
JOM 21229

Reactivity of phosphine–phosphinite complexes. Synthesis and crystal structure of $[\{Ph_2PCH{=}C(O)Ph\}Pd(\mu\text{-}Ph_2PO)]_2$

Dominique Matt

Laboratoire de Chimie Minérale et Analytique, URA 405 CNRS, EHICS, 1 rue Blaise Pascal, F-67008 Strasbourg Cédex (France)

Florent Ingold

Laboratoire de Chimie de Coordination, Université Louis Pasteur, URA 416 CNRS, 4 rue Blaise Pascal, F-67070 Strasbourg Cédex (France)

Fadila Balegroune and Daniel Grandjean

Laboratoire de Cristallochimie, UA 254 CNRS, Université de Rennes I, Avenue du Général Leclerc, F-35042 Rennes Cédex (France)

(Received May 30th, 1990)

Abstract

Treatment of *cis*-$[MCl_2\{Ph_2PCH{=}C(Ph)OPPh_2\}]$ (M = Pd, **1**; Pt, **2**) with 2 equivalents of KOH in dichloromethane yielded quantitatively the dinuclear complexes $[M_2\{Ph_2PCH{=}C(O)Ph\}_2\{\mu\text{-}(Ph_2PO)\}_2]$ (M = Pd, **3**; Pt, **4**). The reaction of KOH with the nickel analogue of **1** led to dissociation of the phosphorus ligands and gave $Ni(OH)_2$. The structure of **3**·toluene was established by an X-ray diffraction study. Crystals of **3**·toluene belong to the space group $P\bar{1}$ with a = 12.76(1) Å, b = 14.672(5) Å, c = 18.657(9) Å, α = 76.97(3)°, β = 68.24(5)°, γ = 75.82(5)°, V = 3110.1 Å^3, and Z = 2. The structure has been refined for 4254 reflections with $F_o^2 > 3\sigma(F_o^2)$ to R = 0.033 and R_w = 0.041. The structure consists of two square planar palladium centers linked together by two Ph_2P–O bridges. The Pd–P(phosphine) bond length are 2.210(2) Å and 2.218(2)Å, and those of the Pd–P(phosphinito) bonds 2.245(2) Å and 2.235(2) Å. The dihedral angle between the metal planes is 72.3° (1) and the six-membered metal ring is in a boat conformation. The P–O bond lengths of 1.533(4) Å and 1.528(4) Å indicate some double bond character. Reaction of complex **1** with 2 equivalents of $NaCo(CO)_4$ gave the trinuclear complex $[\{Ph_2PCH{=}C(Ph)OPPh_2\}PtCo_2(CO)_7]$ (**5**). In contrast to **1** and **2**, the complex **5** does not undergo hydrolytic cleavage of the phosphinite ligand, possibly for steric reasons. All the complexes were characterized by elemental analyses and IR, ^{1}H NMR, and ^{31}P NMR spectroscopy.

Introduction

A number of studies have been concerned with the synthesis and coordination chemistry of anionic $[R_2PO]^-$ ligands (R = alkyl, aryl) [1]. Such ligands are usually generated by one of the three methods depicted in Scheme 1: (a) deprotonation of a coordinated hydroxydialkyl or hydroxydiarylphosphine [2]; (b) ring displacement reaction of metallocenes with dialkyl or diaryl phosphine oxides [3]; basic hydrolysis

0022-328X/90/$03.50

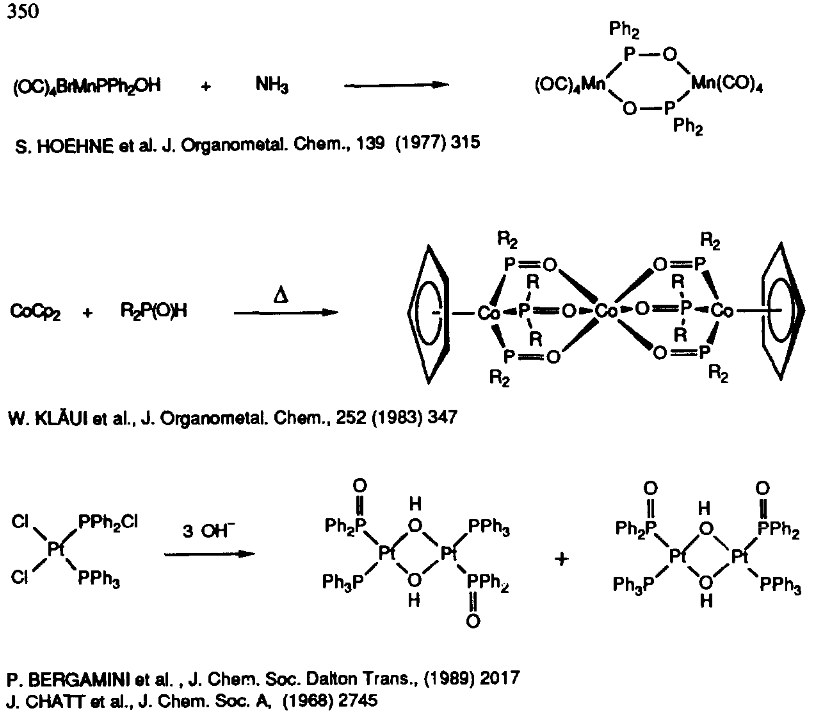

Scheme 1

of coordinated chlorophosphines [4]. An alternative route to such ligands which has been used only occasionally, involves the basic hydrolysis of coordinated phosphinites. In this route there is initial formation of a P–OH group, which is then deprotonated *in situ* by the base present in excess. This method is exemplified by Eq. 1, which depicts the conversion of a functional phosphinite into a mononuclear phosphoranidoxo complex [5]. As an extension of this latter reaction, we describe in this paper reactions of other phosphinite complexes leading to binuclear complexes containing a R_2PO bridge. One such complex, $[\{Ph_2PCH{=}C(O)Ph\}Pd(\mu\text{-}Ph_2PO)]_2$, has been investigated by an X-ray diffraction study.

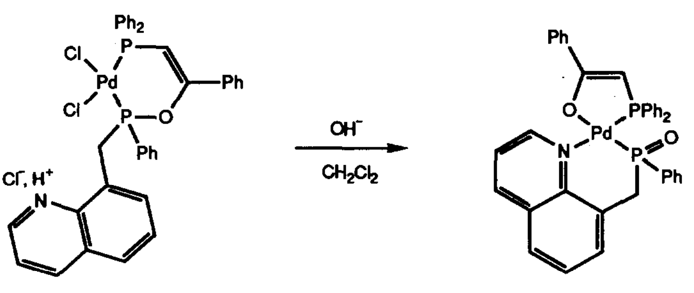

(1)

Results and discussion

Cleavage reaction of a chelating phosphinite

When the complexes *cis*-$[MCl_2\{Ph_2PCH{=}C(Ph)OPPh_2\}]$ (M = Pd, **1**; Pt, **2**) were allowed to react with KOH for several hours at room temperature the binuclear complexes **3** and **4** were obtained quantitatively (Eq. 2):

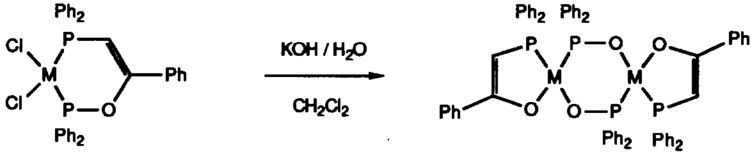

(2)

M = Pd, 1 M = Pd, 3

M = Pt, 2 M = Pt, 4

Characteristic features of these complexes are:

(i) the presence in their IR spectra of two strong absorption bands, at ca. 1520 and 1480 cm^{-1} (ν(C–O) + ν(C=C)), characteristic of the enolate ligand $[Ph_2PCH{=}C(O)Ph]^-$ [6] (for details see Experimental Section).

(ii) small ^2J(PP) coupling constants (< 3 Hz for **3**, 17.5 Hz for **4**), which unambiguously indicate a *cis* PMP arrangement around each metal.

In contrast to reaction 1, the reactions shown in Eq. 2 lead to dinuclear complexes. The formation of complexes **3** and **4** is likely to proceed via nucleophilic attack of OH^- on phosphorus, as shown in Scheme 1. This results in the formation of an enolate fragment and a coordinated hydroxyphosphine. The first of these ligands, $Ph_2PCH{=}C(O)Ph^-$, can easily give a five membered chelate ring by nucleophilic substitution of Cl^-. The second, the hydroxyphosphine, is deprotonated by the base, which is present in excess to give a phosphito complex isolable as a dimer. Although this latter sequence might also produce a complex of the type $[L_nM\{\eta^2\text{-}(R_2P{=}O)\}]$ (see Scheme 1), we have no evidence for the formation of such a transient mononuclear species [7*].

It is noteworthy that Shaw and co-workers have described a similar hydrolytic cleavage of chelating $Ph_2PCH{=}C(Ph)OPPh_2$, which occurred when $[W(CO)_4(Ph_2PCH{=}C(Ph)OPPh_2)]$ was treated with water under UV irradiation (Eq. 3). In this case, however, the hydroxyphosphine formed does not undergo deprotonation but, instead, forms a chelating diphosphine as a result of hydrogen bonding to the neighbouring keto-phosphine [8].

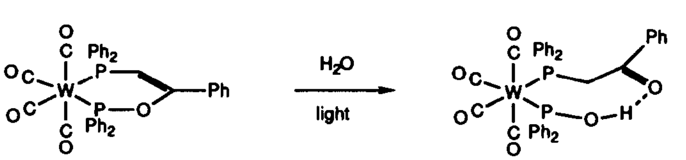

(3)

The review by Walther [1b] makes it clear that R_2PO^- ligands are most frequently coordinated in a terminal fashion (mode **a**) rather than in the bridging mode (**b**).

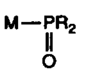

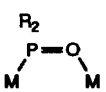

(a) (b)

* A reference number with an asterisk indicates a note in the list of references.

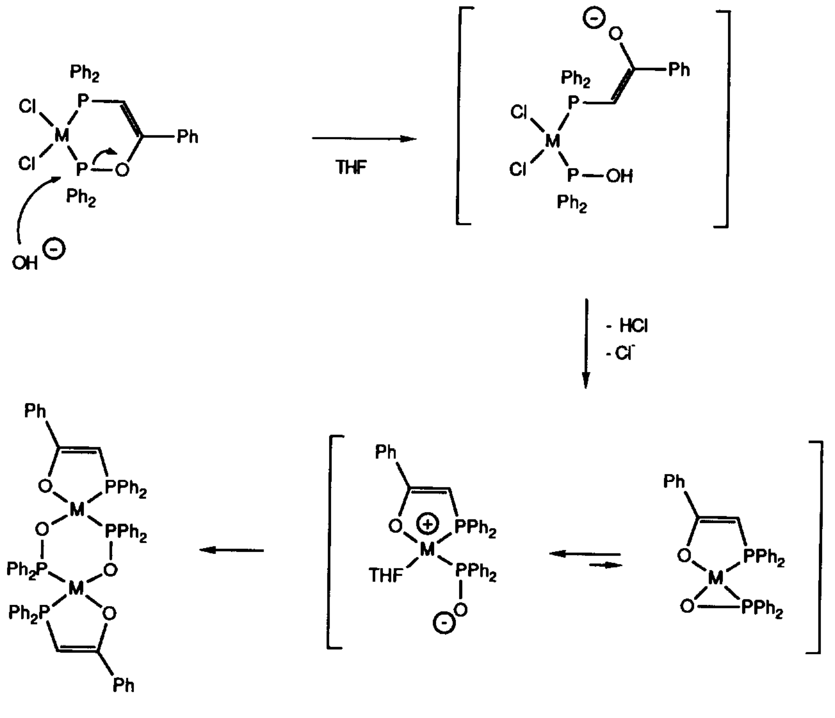

Scheme 2

In reaction 1 form (**a**) is obviously favored over form (**b**) as a result of the presence of a tertiary nitrogen donor atom which allows the formation of a stable chelate complex. This is not possible in the reaction leading to complexes **3** and **4**, and they exist as binuclear species.

Interestingly, treatment of OH^- with *cis*-$[NiCl_2\{Ph_2PCH{=}C(Ph)OPPh_2\}]$ did not give the nickel analogue of **3** but resulted in the quantitative formation of $Ni(OH)_2$. This may be related to the ability of nickel to form tetrahedral complexes, which can readily decompose by dissociation of phosphorus ligands. Such effects are well documented in nickel(II) chemistry [9].

In order to test the stability of the chelating phosphine-phosphinite ligand of **2**, this complex was treated with 2 equivalents of $[NaCo(CO)_4]$ in THF (Eq. 4). This reaction leads quantitatively to the trinuclear complex **5** in which the two chlorine atoms have been substituted by a $Co_2(CO)_7$ fragment. Analytical data for this complex are given in the Experimental Section.

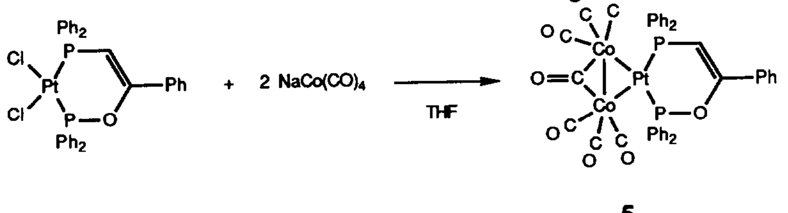

(4)

2 **5**

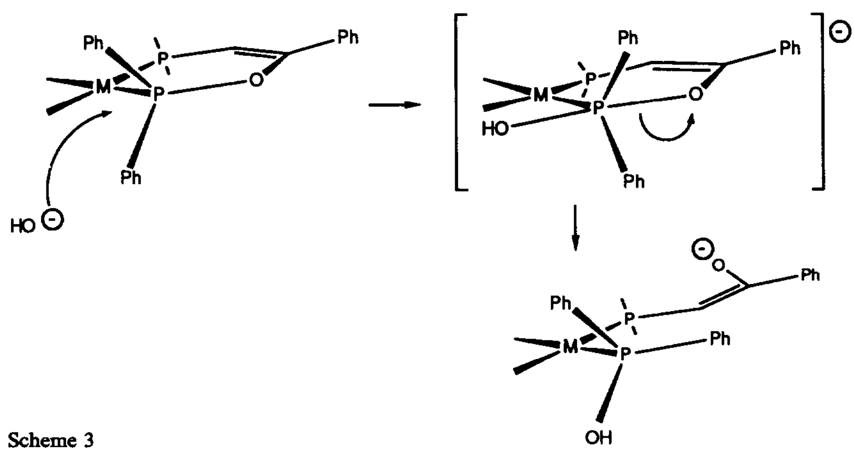

Scheme 3

When a solution of complex **5** was treated with KOH no reaction occured, even upon prolonged heating. The reason for this lies in the fact that during the expected substitution the phosphorus atom would have to adopt a trigonal bipyramidal configuration with leaving and incoming groups in axial positions [10]. This situation can occur, in principle, either after pseudorotation once the P–OH bond is formed or directly if the attack of the hydroxyl group occurs within the cone defined by the P–M bond and the two P–Ph bonds. We believe that in reactions 2 and 3 no pseudo rotation of the intermediate can occur because of the cyclic nature of the phosphorus ligand, which severely limits the freedom of rotation around the phosphorus atom. The nucleophile must therefore approach the phosphorus atom in a roughly "*anti*-PO" direction as shown in Scheme 3. Obviously this condition is satisfied with the chloro complexes **1** and **2** but not with **5**, which contains the bulky $Co(CO)_3$ fragment *cis* to the phosphite phosphorus atom.

X-ray diffraction study of $[\{Ph_2PCH{=}C(O)Ph\}Pd(\mu\text{-}Ph_2PO)]_2 \cdot$ *toluene*

The molecular structure of complex **3** is represented in Fig. 1 together with the atomic numbering scheme. Selected bond distances and angles are given in Table 1. The structure consists of two nominally square planar palladium centers (the maximum deviation from the Pd1–P1–O1–P2–O2 plane is 0.120 Å and that from the Pd2–P3–O3–P4–O4 plane is 0.091 Å) linked together by two Ph_2P–O bridges. The dihedral angle between the metal planes is 72.3°(1). As shown in Fig. 2 the six-membered metal ring is in a boat conformation. This is in contrast to the structures of the other two complexes containing two *anti*-parallel Ph_2P–O bridges which have been determined by X-ray diffraction, namely $[(CO)_4Mn(Ph_2PO)]_2$ and $[(CO_4)Re(Ph_2PO)]_2$. In these complexes the six membered ring adopts a twisted and a chair conformation, respectively [2a,11]. In complex **3** the two M–P–O angles (107.3 and 107.6°) are close to the ideal tetrahedral angle, and the angles around the oxygen atoms O2 and O3 (120.8 and 119.4° respectively) also indicate that there is no particular strain within the six-membered ring. The high values of the Pd1–P2–C23 and Pd2–P3–C41 angles (122.8 and 125.5°, respectively) reflect the

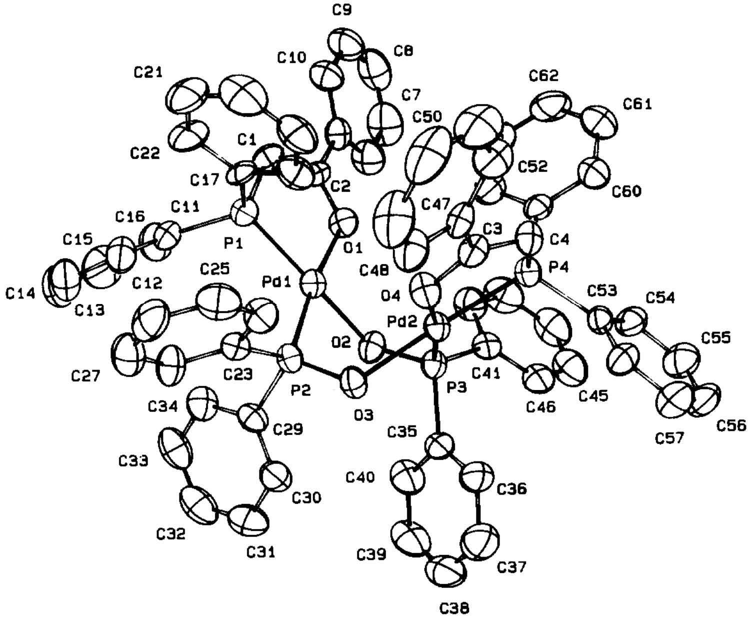

Fig. 1. ORTEP view of $[\{Ph_2PCH{=}C(O)Ph\}Pd(\mu\text{-}Ph_2PO)]_2$ (3)

Table 1

Selected bond distances and angles for complex **3**·toluene

Bond lengths			
Pd1–P1	2.210(2)	Pd2–P4	2.218(4)
Pd1–P2	2.245(2)	Pd2–P3	2.235(4)
Pd1–O1	2.100(4)	Pd2–O4	2.074(4)
Pd1–O2	2.111(4)	Pd2–O3	2.108(4)
P2–O3	1.533(4)	P3–O2	1.528(4)
P1–C1	1.761(7)	P4–C4	1.756(7)
P1–C11	1.816(6)	P4–C53	1.818(7)
P1–C17	1.793(8)	P4–C59	1.816(6)
C1–C2	1.367(9)	C4–C3	1.349(8)
Bond angles			
Pd1–P1–P2	102.19(7)	P4–Pd2–P3	103.54(7)
P1–Pd1–O1	84.0(1)	P4–Pd2–O4	84.1(1)
P1–Pd1–O2	168.8(1)	P4–Pd2–O3	170.7(1)
P2–Pd1–O1	173.3(1)	P3–Pd2–O4	171.6(1)
P2–Pd1–O2	85.7(1)	P3–Pd2–O3	84.3(1)
O1–Pd1–O2	88.5(2)	O4–Pd2–O3	88.4(2)
Pd1–P2–O3	107.6(2)	Pd2–P3–O2	107.3(2)
Pd1–P2–C23	122.8(2)	Pd2–P3–C41	125.5(2)
Pd1–P2–C29	106.5(2)	Pd2–P3–C35	108.4(2)
C23–P2–C29	103.8(3)	C35–P3–C41	102.0(3)
P2–O3–Pd2	119.4(2)	P3–O2–Pd1	120.8(3)

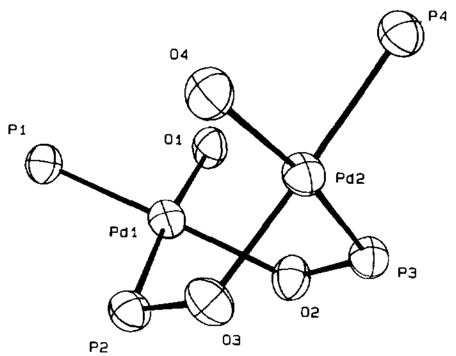

Fig. 2. Partial view of 3 showing the boat conformation of the $Pd_2(\mu\text{-}Ph_2PO)_2$ ring.

steric repulsions between the PPh_2 groups coordinated to the same palladium center. The P–O bond lengths of 1.533(4) and 1.528(4) Å indicate some double bond character. The distances and angles within the phosphino-enolato ligand are similar to those found in other complexes containing this chelating system [12]. Complex 3 crystallized with one toluene molecule (S).

Experimental

General procedures

All reactions were performed in Schlenk-type flasks under dry nitrogen. Dichloromethane and tetrahydrofuran were dried and distilled under nitrogen. The KOH/H_2O solution was degassed before use. Infrared spectra were recorded on a Perkin Elmer 398 spectrophotometer. The ^1H and $^{31}P\{^1H\}$ NMR spectra were recorded, at 200.13 MHz and 81.02 MHz respectively, on a FT-Bruker WP 200 SY instrument. Proton chemical shifts are positive downfield relative to external Me_4Si, and ^{31}P spectra were externally referenced to 85% H_3PO_4 in H_2O with downfield chemical shifts reported as positive. The complexes $[MCl_2\{Ph_2PCH{=}C(Ph)OPPh_2\}]$ were prepared as described previously [13].

$[Pd_2\{Ph_2PCH{=}C(O)Ph\}_2\{\mu\text{-}(Ph_2PO)\}_2](3)$

A solution of KOH (0.061 g, 1.08 mmol) in H_2O (2 mL) was added to a solution of $[PdCl_2\{Ph_2PCH{=}C(Ph)OPPh_2\}]$ (0.360 g, 0.54 mmol) in CH_2Cl_2 (30 mL) and the yellow mixture obtained was stirred for 12 h after which both solvents, dichloromethane and water, were removed in vacuo. The residue was treated with 15 mL of water in order to dissolve KCl and unreacted KOH. The suspension thus obtained was filtered and the filtered product dried in high vacuum. It then was dissolved in CH_2Cl_2 and n-pentane was added affording a yellow powder. Recrystallization from dichloromethane/n-pentane at $-15\,°C$ gave the product as yellow crystals (0.297 g, 90%). Anal. Found: C 63.09, H 4.41. $C_{64}H_{52}O_4P_4Pd_2$ (M_r = 1221.81) calcd.: IR(KBr): 1520 s, 1485 s cm^{-1}. ^1H NMR ($CDCl_3$): δ 4.72 (dd, 2H, PCH, $^2J(PH)$ = 5.3 Hz, $^4J(PH)$ = 1.8 Hz), 6.92–8.10 (25H, aromatic H) ppm. $^{31}P\{^1H\}$ NMR(CH_2Cl_2–C_6D_6): δ 39.2 (s, Ph_2PCH, $^2J(PP)$ = 0 Hz), 88.0 (s, Ph_2P–O) ppm.

$[Pt_2\{Ph_2PCH{=}C(O)Ph\}_2\{\mu\text{-}(Ph_2PO)\}_2]$ (4)

To a solution of $[PtCl_2\{Ph_2PCH{=}C(Ph)OPPh_2\}]$ (0.420 g, 0.56 mmol) in CH_2Cl_2 (30 ml) was added a solution of KOH (0.078 g, 1.40 mmol) in H_2O (2 ml). After 12 h stirring, the solvents dichloromethane and water were removed in vacuo and the residue washed several times with water. The aqueous solution was separated from the white product using a glass pipette. The product was then dried in vacuo. Recrystallization from toluene/pentane gave the complex as colourless crystals (0.360 g, 92%). Anal. Found: C 54.87, H 3.80. $C_{64}H_{52}O_4P_4Pt_2$ ($M_r = 1399.17$) calcd.: C 54.94, H 3.75%. IR(KBr): 1518 s, 1482 s cm^{-1}. ^1H NMR ($CDCl_3$): δ 4.90 (dd with Pt satellites, 2H, $^2J(PH) = 8.3$ Hz, $^4J(PH) = 1.5$ Hz, $^3J(PtH) = 42$ Hz, 6.89–8.10 (25 H, aromatic H) ppm. $^{31}P\{^1H\}$ NMR(CH_2Cl_2–C_6D_6): δ 12.2 (d with Pt satellites, PCH, $^2J(PP) = 18$ Hz, $J(PPt) = 4140$ Hz), 59.9 (dd with Pt satellites, P–O, $^2J(PP) = 18$ Hz, $J(PPt) = 3611$ Hz) ppm.

Table 2

Crystal data and data collection of **3**

formula	$C_{64}H_{52}O_4P_4Pd_2 \cdot$ toluene
f.w.	1313.99
cryst. system	triclinic
space group	$P\bar{1}$
a, Å	12.76(1)
b, Å	14.672(5)
c, Å	18.657(9)
α, deg	76.97(3)
β, deg	68.24(5)
γ, deg	75.82(5)
V, Å^3	3110.1
Z	2
ρ(calcd), g cm^{-3}	1.403
cryst. dimens., mm	$0.22 \times 0.18 \times 0.09$
$F(000)$	1340
systematic absences	none
diffractometer	Enraf–Nonius CAD-4
radiation (graphite monochromator)	Mo-K_α ($\lambda = 0.71073$)
linear abs. coeff., cm^{-1}	7.179
scan type	$\omega/2\theta$
scan range, deg	$1 + 0.35 \tan\theta$
θ limits, deg	1–25
octants coll.	$+h, \pm k, \pm l$
no. of data coll.	7909
no. of unique data used	4254 ($F_o^2 > 3\sigma(F_o^2)$)
no. of variables	696
decay, %	<1%
$R = \Sigma(\|\|F_o\| - \|F_c\|\|)/\Sigma\|F_o\|$	0.033
$R_w = [\Sigma w(\|F_o\| - \|F_c\|)^2/\Sigma w\|F_o\|^2]^{1/2}$	0.041
$GOF = [\Sigma w(\|F_o\| - \|F_c\|)^2/(N_{obs} - N_{var})]^{1/2}$	1.214
largest shift/esd, final cycle	0.0
largest peak, e Å^{-3}	0.57
fudge factor	0.05

Table 3

Fractional atomic coordinates and temperature parameters for compound 3·toluene

Atom	x	y	z	$B(Å^2)$ [a]
Pd1	0.21174(4)	0.37712(4)	0.32981(3)	2.83(1)
Pd2	0.29965(4)	0.21600(3)	0.21072(3)	2.68(1)
P1	0.3226(2)	0.4429(1)	0.36252(9)	3.09(5)
P2	0.2393(2)	0.2265(1)	0.38912(9)	2.87(5)
P3	0.1124(2)	0.2761(1)	0.24149(9)	2.87(5)
P4	0.3660(2)	0.2525(1)	0.08178(9)	2.85(5)
O1	0.1800(4)	0.5118(3)	0.2655(2)	3.4(1)
O2	0.0820(4)	0.3383(3)	0.3044(2)	3.4(1)
O3	0.2570(4)	0.1611(3)	0.3306(2)	3.3(1)
O4	0.4705(3)	0.1622(3)	0.1987(2)	3.3(1)
C1	0.3049(5)	0.5582(4)	0.3101(4)	3.3(2)
C2	0.2323(5)	0.5742(4)	0.2683(3)	3.0(2)
C3	0.5436(5)	0.1702(4)	0.1274(3)	3.0(2)
C4	0.5125(5)	0.2057(5)	0.0635(3)	3.0(2)
C5	0.2088(6)	0.6707(5)	0.2212(3)	3.5(2)
C6	0.1103(7)	0.6940(5)	0.2025(4)	4.9(2)
C7	0.0823(7)	0.7842(6)	0.1624(5)	6.5(3)
C8	0.1520(8)	0.8485(6)	0.1407(4)	6.5(3)
C9	0.2522(7)	0.8247(5)	0.1582(4)	5.9(3)
C10	0.2798(7)	0.7364(5)	0.1993(4)	4.8(2)
C11	0.2683(6)	0.4516(4)	0.4660(3)	3.3(2)
C12	0.3144(6)	0.3893(5)	0.5196(4)	4.4(2)
C13	0.2609(7)	0.3917(6)	0.5987(4)	6.3(3)
C14	0.1601(8)	0.4545(7)	0.6248(4)	7.6(3)
C15	0.1148(8)	0.5171(6)	0.5732(5)	7.0(3)
C16	0.1695(7)	0.5157(5)	0.4931(4)	5.1(2)
C17	0.4742(5)	0.4000(4)	0.3349(3)	2.8(2)
C18	0.5277(6)	0.3494(5)	0.2732(4)	4.3(2)
C19	0.6459(7)	0.3249(6)	0.2463(4)	4.9(2)
C20	0.7129(6)	0.3491(6)	0.2792(5)	5.8(3)
C21	0.6604(7)	0.4015(6)	0.3415(5)	6.0(3)
C22	0.5395(6)	0.4256(5)	0.3689(4)	4.5(2)
C23	0.3519(6)	0.1793(4)	0.4312(3)	3.1(2)
C24	0.4603(6)	0.1530(5)	0.3802(4)	3.8(2)
C25	0.5516(7)	0.1187(6)	0.4082(4)	5.3(3)
C26	0.5383(6)	0.1077(5)	0.4854(4)	5.3(2)
C27	0.4264(7)	0.1317(6)	0.5371(4)	5.0(2)
C28	0.3361(6)	0.1679(5)	0.5097(4)	4.1(2)
C29	0.1092(6)	0.2121(5)	0.4709(3)	3.2(2)
C30	0.0512(6)	0.1417(5)	0.4787(4)	4.1(2)
C31	−0.0495(7)	0.1307(6)	0.5409(4)	5.5(3)
C32	−0.0898(7)	0.1900(6)	0.5959(4)	5.5(3)
C33	−0.0323(7)	0.2613(6)	0.5900(4)	5.2(2)
C34	0.0677(6)	0.2738(5)	0.5260(4)	4.1(2)
C35	0.0332(6)	0.1783(5)	0.2823(4)	3.3(2)
C36	0.0752(6)	0.0916(5)	0.2552(4)	4.4(2)
C37	0.0103(7)	0.0192(6)	0.2880(4)	6.0(3)
C38	−0.0934(7)	0.0336(6)	0.3476(4)	6.4(3)
C39	−0.1325(6)	0.1191(7)	0.3734(4)	5.8(3)
C40	−0.0715(6)	0.1918(6)	0.3416(4)	4.8(2)
C41	0.0413(5)	0.3478(5)	0.1734(3)	3.0(2)
C42	0.0211(6)	0.4445(5)	0.1688(4)	4.6(2)

Table 3 (continued)

Atom	x	y	z	$B(\AA^2)$ [a]
C43	−0.0439(7)	0.5010(6)	0.1249(5)	5.7(3)
C44	−0.0897(7)	0.4599(6)	0.0854(4)	5.9(3)
C45	−0.0680(7)	0.3637(6)	0.0896(4)	5.3(2)
C46	−0.0051(6)	0.3074(5)	0.1335(4)	3.9(2)
C47	0.6652(5)	0.1348(4)	0.1235(3)	3.1(2)
C48	0.6915(6)	0.0732(5)	0.1859(4)	4.3(2)
C49	0.8043(6)	0.0426(6)	0.1841(4)	5.9(3)
C50	0.8926(7)	0.0730(6)	0.1203(5)	6.4(3)
C51	0.8680(7)	0.1317(6)	0.0591(5)	5.8(3)
C52	0.7572(6)	0.1640(5)	0.0602(4)	4.5(2)
C53	0.3121(5)	0.1926(4)	0.0309(3)	2.8(2)
C54	0.2314(6)	0.2395(5)	−0.0043(4)	3.7(2)
C55	0.1860(6)	0.1917(6)	−0.0378(4)	5.0(2)
C56	0.2248(7)	0.0939(5)	−0.0368(4)	5.4(2)
C57	0.3060(7)	0.0473(5)	−0.0033(4)	5.3(2)
C58	0.3512(6)	0.0951(5)	0.0298(4)	4.2(2)
C59	0.3580(5)	0.3751(4)	0.0338(3)	2.9(2)
C60	0.4075(6)	0.3925(5)	−0.0468(4)	4.2(2)
C61	0.4125(7)	0.4849(5)	−0.0843(4)	5.1(2)
C62	0.3703(7)	0.5593(5)	−0.0418(5)	5.4(2)
C63	0.3218(7)	0.5429(5)	0.0371(4)	5.3(2)
C64	0.3161(6)	0.4499(5)	0.0764(4)	4.2(2)
C1S	0.379(1)	0.712(1)	0.4339(8)	14.9(5) [b]
C2S	0.4221(8)	0.7712(7)	0.3572(5)	7.1(2) [b]
C3S	0.3751(8)	0.8668(7)	0.3524(6)	8.1(3) [b]
C4S	0.4100(9)	0.9287(8)	0.2849(6)	10.0(3) [b]
C5S	0.490(1)	0.8868(9)	0.2266(7)	11.1(4) [b]
C6S	0.540(1)	0.7975(9)	0.2273(7)	11.3(4) [b]
C7S	0.508(1)	0.7328(9)	0.2945(6)	10.6(4) [b]

[a] Anisotropic parameters are given in the form of the isotropic equivalent displacement parameter defined as $4/3\,[a^2B_{1,1}+b^2B_{2,2}+c^2B_{3,3}+ab(\cos\gamma)B_{1,2}+ac(\cos\beta)B_{1,3}+bc(\cos\alpha)B_{2,3}]$. [b] Refined isotropically.

[{$Ph_2PCH{=}C(Ph)OPPh_2$}$PtCo_2(CO)_7$] (5)

A solution of $NaCo(CO)_4$ (0.388 g, 2.0 mmol) in THF (20 ml) was added dropwise at −78°C to a solution of [$PtCl_2${$Ph_2PCH{=}C(Ph)OPPh_2$}] (0.755 g, 1.0 mmol) in THF (20 ml). The mixture was stirred for 12 h at room temperature and the solvent then removed in vacuo. The residue was extracted with toluene and the resulting solution filtered. Addition of n-pentane gave dark red crystals of the complex (0.828 g, 75%). Anal. Found: C 46.90, H 2.61. $C_{39}H_{26}Co_2O_8P_2Pt$ (M_r = 997.54) calcd.: C 46.96, H 2.63%. MS (ZAB, matrix 1,3-dinitrobenzylalcohol): 997.9 (9%), 912.9 (100%). IR (THF): 1962 s br cm^{-1}. IR (KBr): 2047 w, 2007 m, 1992 sh, 1973 s cm^{-1}. ^1H NMR ($CDCl_3$): δ 6.15 (d with Pt satellites, 1 H, PCH, $^2J(PH)$ = 1.9 Hz, $J(PtH)$ = 44.3 Hz). $^{31}P\{^1H\}$ NMR (THF/C_6D_6): δ −3.3 (dd with Pt satellites, Ph_2PC, $^2J(PP)$ = 56 Hz, $J(PPt)$ = 3112 Hz), 118.0 (dd with Pt satellites, Ph_2PO, $^2J(PP)$ = 56 Hz, $J(PPt)$ = 3888 Hz).

Crystal structure determination of [$Pd_2\{Ph_2PCH=C(O)Ph\}_2\{\mu\text{-}(Ph_2PO)\}_2$] · toluene (3)

Pale yellow crystals of **3** · toluene were obtained by slow diffusion of n-pentane into a dichloromethane–toluene solution of the complex. All data were collected at room temperature (23 ± 2° C). Precise lattice parameters were determined by standard Enraf–Nonius least-squares methods using 25 carefully selected reflections. Intensity data were collected on an automated four-circle diffractometer. No intensity decay was observed during the data collection period. For all subsequent computations the Enraf–Nonius SDP was used [14]. Intensities were corrected for Lorentz-polarization. Absorption corrections were omitted in view of the low linear absorption coefficient. The crystal structure was solved by using the Patterson and Fourier difference methods and refined by full matrix least squares with anisotropic thermal parameters for all non-hydrogen atoms. The function minimized was $\Sigma (w|F_o| - |F_c|)^2$, where the weight w is $[1/4\ ((\sigma^2(I)/I + (0.05\ I)^2/I)]^{-1}$. Hydrogen atoms were place in calculated positions (C–H distance = 0.95 Å) in structure factor calculations and were assigned isotropic thermal parameters of $B = 5.0$ Å^2. The neutral-atom scattering factors used for all atoms and anomalous scattering factors for all non-hydrogen atoms were obtained from ref. 15. Results of the refinement are given in Table 2. Atomic coordinates with estimated standard deviations corresponding to the final least-squares refinement cycle are given in Table 3. A list of hydrogen atom coordinates, a table anisotropic thermal parameters for non-hydrogen atoms, a complete table of bond distances and angles, a list of observed and calculated structure factor amplitudes, and a list of selected least-squares planes are available from the authors.

Acknowledgements

D.M. is grateful to Dr. P. Braunstein for his interest in this work and for his stimulating comments. We thank Dr. L. Cullen for his comments on the manuscript and the CNRS for financial support.

References

1 See for example: (a) D.E. Berry, K.A. Beveridge, G.W. Bushnell, K.R. Dixon and A. Pidcock, Can. J. Chem., 64 (1986) 343; (b) B. Walther, Coord. Chem. Rev., 60 (1984) 67; (c) D.M. Roundhill, R.P. Sperline and W.B. Beaulieu, Coord. Chem. Rev., 26 (1978) 263.
2 See for example: (a) S. Hoehne, E. Lindner and B. Schilling, J. Organomet. Chem., 139 (1977) 315; (b) K.R. Dixon and A.D. Rattray, Can. J. Chem., 49 (1971) 3997.
3 W. Kläui, W. Eberspach and R. Schwarz, J. Organomet. Chem., 252 (1983) 347.
4 (a) P.M. Treichel and L.D. Rosenheim, Inorg. Chem., 20 (1981) 1539; (b) P. Bergamini, S. Sostero, O. Traverso, T.J. Kemp and P.G. Pringle, J. Chem. Soc. Dalton Trans., (1989) 2017; (c) J. Chatt and B.T. Heaton, J. Chem. Soc. A, (1968) 1745.
5 F. Balegroune, P. Braunstein, D. Grandjean, D. Matt and D. Nobel, Inorg. Chem., 27 (1988) 3320.
6 S.-E. Bouaoud, P. Braunstein, D. Grandjean, D. Matt and D. Nobel, Inorg. Chem., 25 (1986) 3765.
7 To date no $\eta^2(P, O)$ coordinated R_2PO^- ligand has been characterized. Mononuclear [$L_nM\{\eta^2\text{-}(R_2P{=}S)\}$] are known: see for example E. Lindner, B. Bouachir and S. Hoehne, Chem. Ber., 116 (1983) 46.
8 S. Al-Jibori, M. Hall, A.T. Hutton and B.L. Shaw, J. Chem. Soc., Dalton Trans., (1984) 863.
9 G.R. Van Hecke and W.D. Horrocks, Inorg. Chem., 5 (1966) 1968.
10 A.F. Holleman and N. Wiberg, in Lehrbuch für Anorganische Chemie, De Gruyter, 1984, p. 640.

11 G. Munding, B. Schilling, M. Weishaupt, E. Lindner and J. Strähle, Z. Anorg. Allg. Chem., 437 (1977) 169.
12 H. Quichen, X. Minzhi, Q. Yanlong, X. Weihua, S. Meicheng and T. Youqi, J. Organomet. Chem., 287 (1985) 419.
13 P. Braunstein, D. Matt, D. Nobel, F. Balegroune, S.-E. Bouaoud, D. Grandjean and J. Fischer, J. Chem. Soc., Dalton Trans., (1988) 353.
14 B.A. Frenz in H. Schenk, R. Olthof-Hazekamp, H. Van Koningsveld and G.C. Bassi (Eds.), The Enraf-Nonius CAD4-SDP, Computing in Crystallography; University Press, Delft, The Netherlands, 1979, p. 64–71.
15 International Tables for X-ray Crystallography; Kynoch, Birmingham, England, Vol. IV, 1974, p. 99.